Electronic Supplementary Material (ESI) for Journal of Materials Chemistry C.

(Supporting Information)

Bias Stability Improvement of Oxyanion Incorporated Aqueous Sol-gel Processed Indium Zinc Oxide TFT

Hyungjin Park†, Yun-Yong Nam†, Jungho Jin and Byeong-Soo Bae*

Laboratory of Optical Materials and Coating (LOMC), Department of Materials Science and Engineering, Korea Advanced Institute of Science and Technology (KAIST), Daejeon 305-701, Korea

*corresponding author. E-mail address: bsbae@kaist.ac.kr

† Both authors contributed equally to this work.

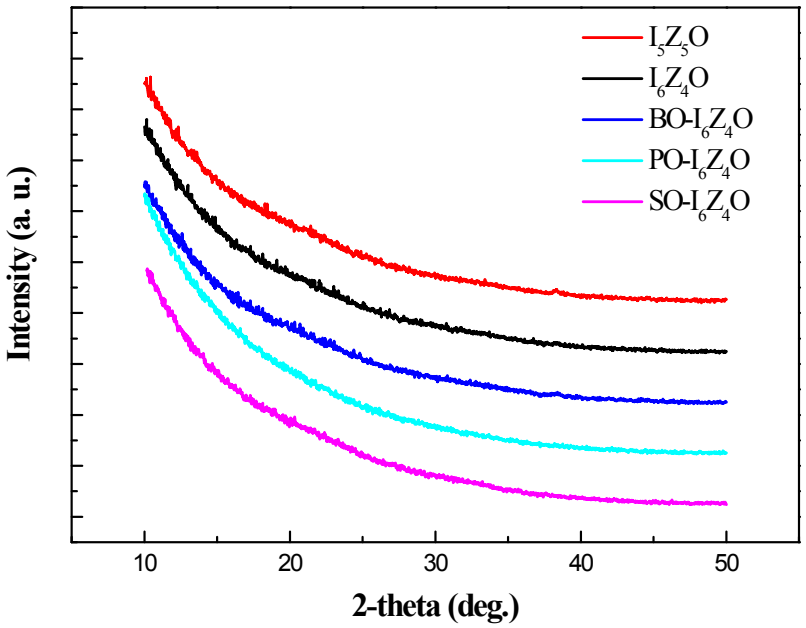

Figure S1 XRD patterns of IZO and inorganic incorporated IZO thin films. The power of X-ray source was 40 kV and 300 mA and the patterns were obtained using 2-theta scan (theta=2°, scan speed=2 °/min).

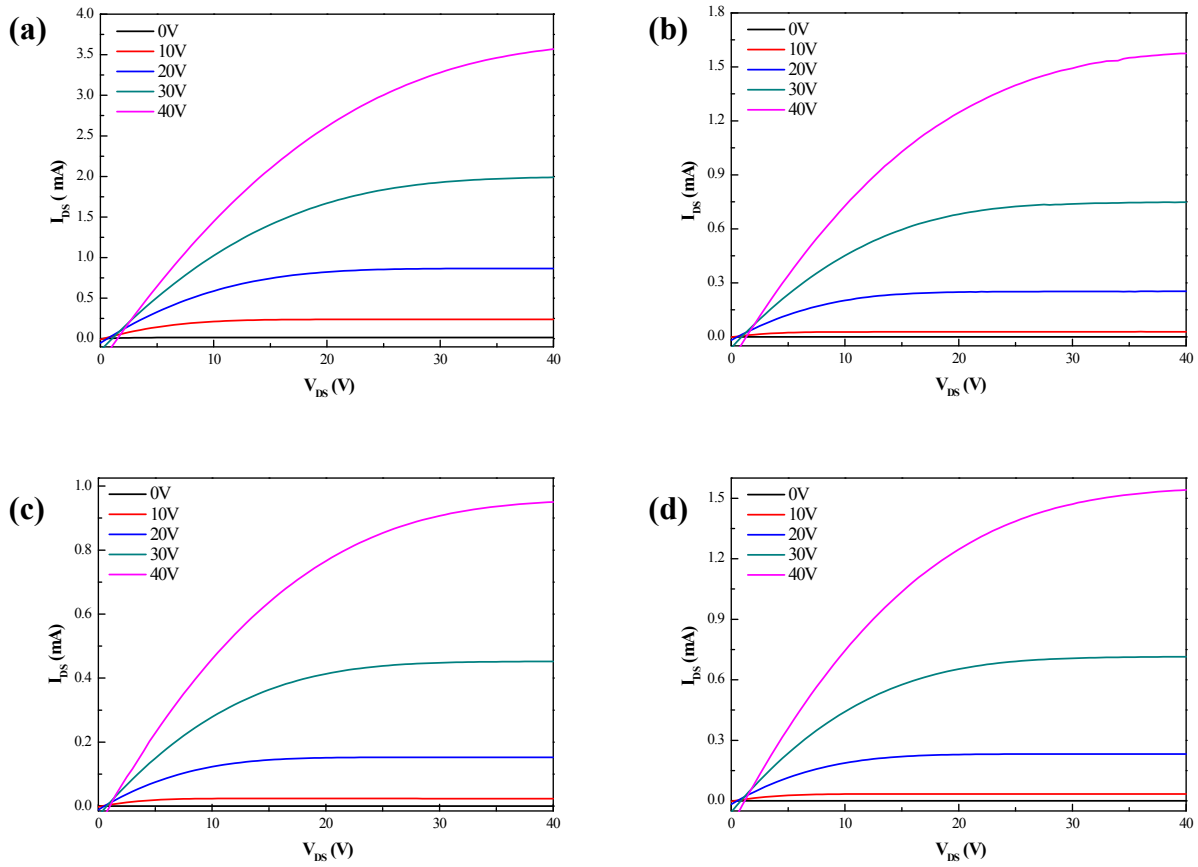

Figure S2 Output curves of (a) I_6Z_4O (b) SO-, (c) PO-, and (d) BO-I_6Z_4O TFTs as a function of applied gate bias (V_G= 0, 10, 20, 30 and 40 V). All the output curve characteristics show the saturation behavior and incorporation of oxyanion result in decrease of overall current level.

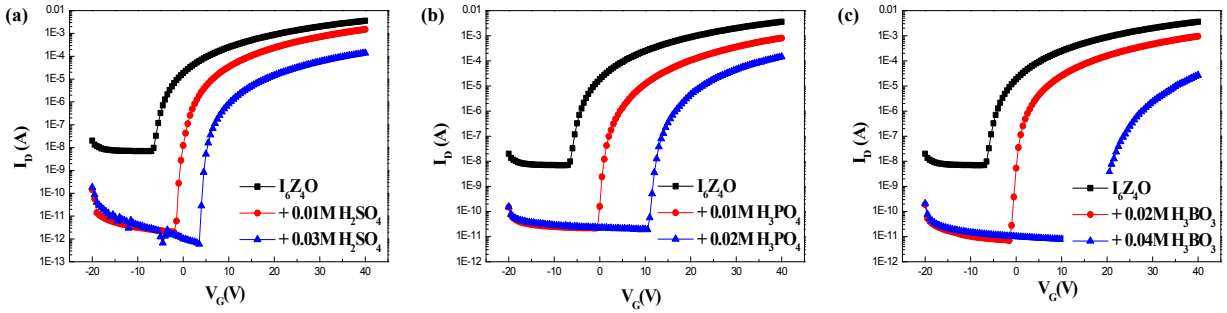

Figure S3 Transfer characteristics of (a) sulfuric, (b) phosphoric and (c) boric acid incorporated indi um zinc oxide TFT according to the various composition.

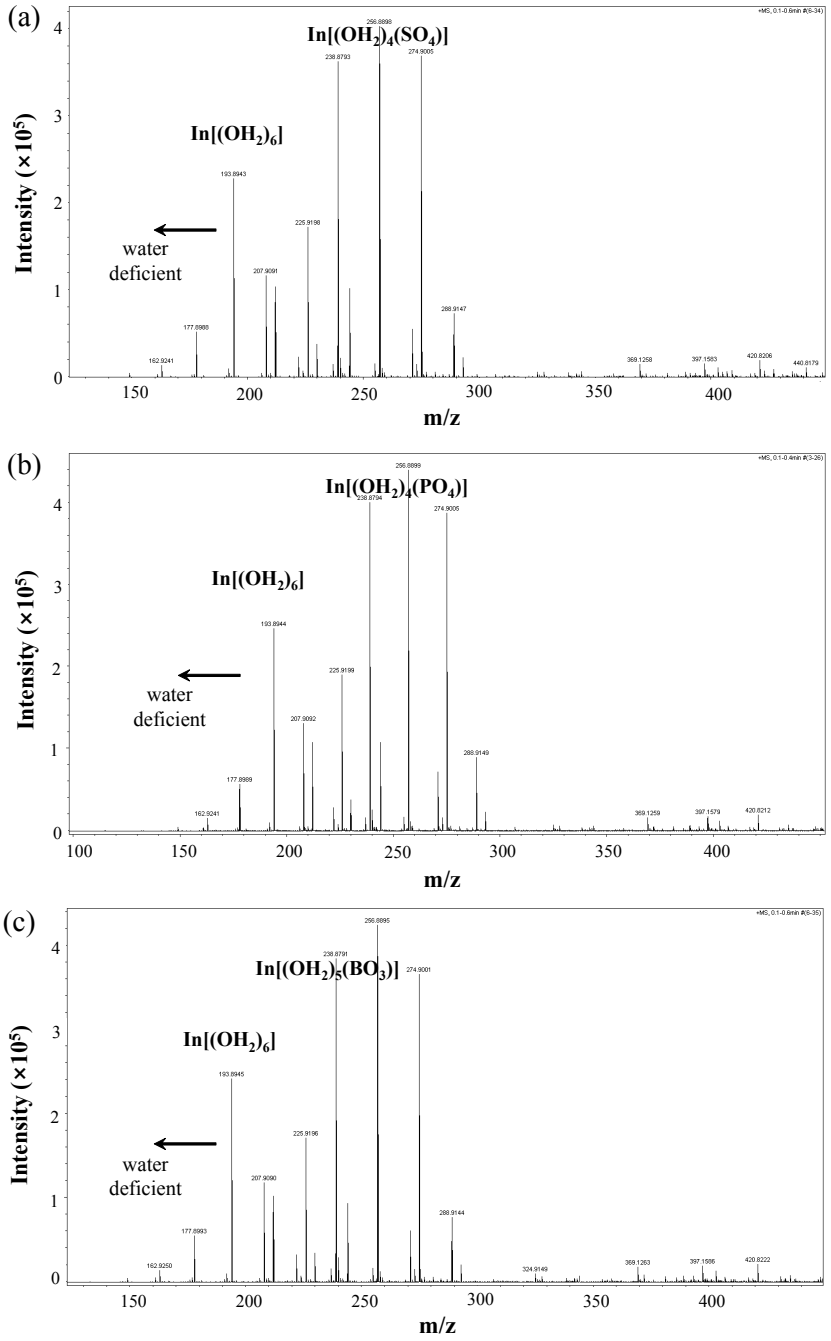

Figure S4 HR-MS (high-resolution mass spectrometry; electrospray ionization) analyses of (a) sulfuric acid (b) phosphoric acid and (c) boric acid incorporated aqueous indium nitrate solution. Hwang et al. reported that a hexa-aquo indium complex ($[In(OH_2)_6]$) is formed in aqueous indium nitrate solution.[9] Variation in the number of surrounding aquo ligands of the complex results in an interval of 18 m/z identical to molecular weight of aquo ligand.[12] Incorporation of sulfate (SO_4^{2-}, M_w=96), phosphate (PO_4^{3-}, M_w=94) and borate (BO_3^{3-}, M_w=58) replaces some of aquo ligands and heavier molecular species are observed.

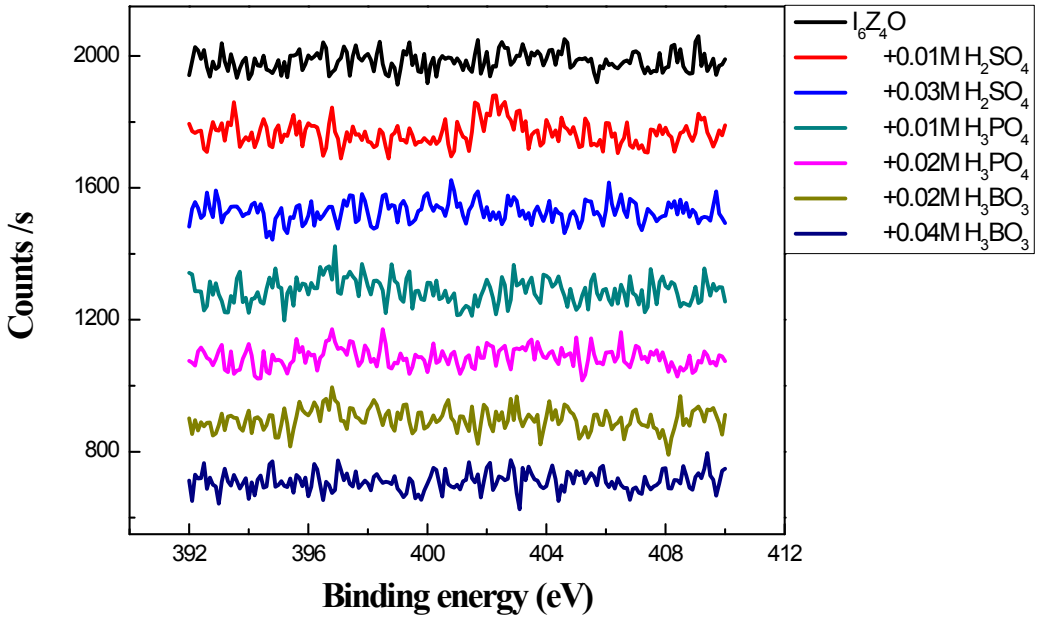

Figure S5 XPS N 1s spectra of oxyanion incorporated I_6Z_4O thin films. All the thin films are nitroge n-free after thermal annealing.

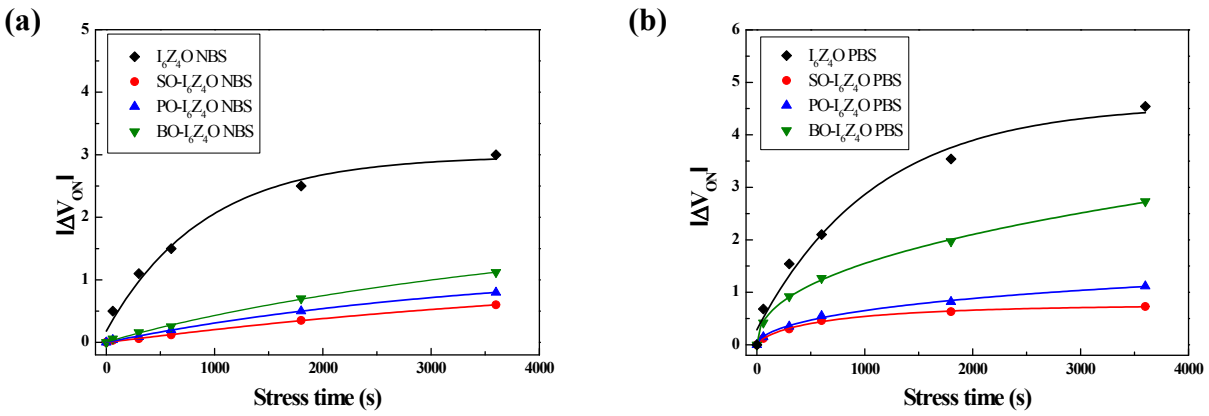

Figure S6 V_{ON} shift under (a) NBS and (b) PBS conditions fitted with stretched exponential equation.

Precursor composition					Atomic ratio				
$In(NO_3)_3 \cdot xH_2O$	$Zn(NO_3)_2 \cdot xH_2O$	H_2SO_4	H_3PO_4	H_3BO_3	In	Zn	S	P	B
0.12 M	0.08 M	-	-	-	62.9 %	37.1 %	-	-	-
0.12 M	0.08 M	0.01M	-	-	61.3 %	33.1 %	5.6 %	-	-
0.12 M	0.08 M	0.03M	-	-	56.4 %	34.1 %	9.5 %	-	-
0.12 M	0.08 M	-	0.01M	-	58.0 %	37.8 %	-	4.2 %	-
0.12 M	0.08 M	-	0.02M	-	56.3 %	33.4 %	-	10.3 %	-
0.12 M	0.08 M	-	-	0.02M	52.7 %	37.2 %	-	-	10.0 %
0.12 M	0.08 M	-	-	0.04M	51.1 %	29.3 %	-	-	19.6 %

Table S1. The chemical composition of precursor solutions and the atomic ratio of resulting films cal culated from XPS analysis.